Molecular Organization and Motions of Crystalline Monoacylglycerols and Diacylglycerols: A C-13 MASNMR Study

Wen Guo and James A. Hamilton
Biophysics Department, Boston University School of Medicine, Boston, Massachusetts 02118-2394

ABSTRACT Six saturated acylglycerols (1-myristoyl-*sn*-glycerol, 1-palmitoyl-*sn*-glycerol, 1,2-dimyristoyl-*sn*-glycerol, 1,2-dipalmitoyl-*sn*-glycerol, 1,2-dipalmitoyl-rac-glycerol, and 1,3-dimyristoylglycerol) were studied in their various polymorphic forms (sub-α, α, β') by natural abundance C-13 nuclear magnetic resonance (NMR) with magic angle spinning (MASNMR). C-13 MASNMR does not require single crystals and can observe relatively disordered crystals, distinct advantages over crystallographic diffraction methods. Well resolved spectra were obtained for each acylglycerol, and the chemical shifts of corresponding carbons were different for each crystalline phase and the isotropic liquid phase; moreover, in the case of monoacylglycerols, the symmetrically nonequivalent molecules in the same crystalline structure gave distinct C-13 resonances for the same carbon. The C-13 chemical shifts corresponding to each polymorphic phase were interpreted in terms of differences in intramolecular bond distances, intermolecular interactions (such as H bonding), and molecular motions. Mobilities of the glycerol backbone and acyl chains were assessed by the C-13 linewidths and the C—H dipolar relaxation rates. The chemical shift anisotropy(ies) ($\Delta\sigma$) of the carbonyl group(s) of each acylglycerol was determined from slow-spinning MAS spectra, and was discussed in terms of the conformational and/or motional changes for the carbonyl carbon(s).

INTRODUCTION

Acylglycerols are a complex class of lipids composed of fatty acids esterified to glycerol. They are important molecules in physiology, acting as storage forms of fat or intermediates in lipid metabolism. Diacylglycerols have attracted special interest because of their role in cellular signal transduction by activating protein kinase C, an event that takes place in the plasma membrane (Ganong et al., 1986). Low levels of 1,2-diacylglycerol incorporate into phosphatidylcholine bilayers and adopt a conformation that is similar to the host phospholipid and different from the glycerol conformation in its own β' crystalline state (Hamilton et al., 1991; Smith et al., 1992). Diacylglycerols can disrupt the lamellar structure of phospholipid bilayers to form a hexagonal phase (Siegel et al., 1989; Epand et al., 1988; de Boeck and Zidovetzki, 1992). In unusual cases in nature such as the insect lipoprotein lipophorin, diacylglycerols exist in a separated diacylglycerol-rich phase (Soulages et al., 1994).

Acylglycerols exist in a variety of polymorphic forms, among which β' and α forms are the most commonly encountered (Chapman, 1962; Larsson, 1966a,b; Pascher et al., 1981; Small, 1986; Dorset and Pangborn, 1988; Di and Small, 1993). Complete understanding of the properties of acylglycerols in biological systems, such as molecular interactions and conformations, requires knowledge of the molecular arrangements of acylglycerols in their polymorphic states. Various acylglycerols have been studied by calorimetry and x-ray diffraction (Small, 1986); however, only a few acylglycerols in their β' forms have been determined by single-crystal x-ray diffraction or electron diffraction (Larsson, 1966b; Hybl and Dorset, 1971; Dorset and Pangborn, 1988; Pascher et al., 1981). From the limited structural data, it is believed that the molecular conformations in the crystalline structure are strongly dependent on the number and position of the acyl chains, and less so on chain length.

C-13 magic angle spinning nuclear magnetic resonance (MASNMR) is a powerful method for the study of ordered phases of lipids that is complementary to crystallographic method and provides details of molecular organization, conformation, and interactions in crystalline lipids (Hamilton et al., 1991b; Norton et al., 1985; Bociek et al., 1985; Guo and Hamilton, 1993). C-13 MASNMR has the important advantage that single crystals are not required, and solids with considerable disorder can be studied. Quantitative information about molecular motions not obtainable with crystallographic methods can also readily be obtained with MASNMR.

In the present work, C-13 MASNMR is used to study the polymorphism of four diacylglycerols (1,2-dimyristoyl-*sn*-glycerol (d-DMG), 1,2-dimyristoyl-rac-glycerol (r-DMG), 1,2-dipalmitoyl-*sn*-glycerol (DPG) and 1,3-dimyristoylglycerol (1,3DMG)) and two monoacylglycerols (1-myristoyl-*sn*-glycerol (MMG) and 1-palmitoyl-*sn*-glycerol (MPG)). These six acylglycerols each exhibit at least two crystalline phases (α and β'). Unambiguous crystal structures have been reported only for the β' phase of DPG (Pascher et al., 1981). Bromine-substituted analogues of 1,3DMG (Hybl and Dorset, 1971) and 1-mono-*sn*-undecanylglycerol in the β' phase were reported as structural models for the corresponding acylglycerols. We obtained high-resolution C-13 spectra of each solid state of all these acylglycerols in various polymorphic forms by the standard

Received for publication 22 June 1994 and in final form 20 December 1994.
Address reprint requests to Dr. James A. Hamilton, Department of Biophysics, Boston University School of Medicine, Center for Advanced Biomedical Research W302, 80 E. Concord Street, Boston, MA 02118-2394. Tel.: 617-638-5048; Fax: 617-638-4041; E-mail: hamilton@med-biophd.bu.edu.

0006-3495/95/04/1383/13 $2.00

cross-polarization (CP) transfer with magic angle sample spinning (CPMAS). Differential internal mobilities were studied by linewidth measurements and by dephased CP-MAS. To study molecular conformations, the chemical shift anisotropies of the carbonyl carbons were measured by slow spinning CPMAS. The relationship between the C-13 spectroscopic measurements and the molecular structures and mobilities is discussed.

MATERIALS AND METHODS

MMG, and MPG, d-DMG, r-DMG, DPG, and 1,3DMG were purchased from Serdary Research Laboratory, Inc. (Port Huron, MI). Samples were received as polycrystalline powder recrystallized from hexane. The purity was checked by thin-layer chromatography TLC (chloroform:methanol, 97:3). There were no observable impurities found for MMG, MPG, and 1,3DMG before and after the NMR experiments. About 2–3% 1,3 isomers were found in d-DMG, DPG and r-DMG before and about 5% after the NMR experiments. No further purification was performed on any samples used in the current work.

MASNMR measurements were performed on a Bruker (Billerica, MA) AMX-300 (75 MHz for C-13, 7.05 T) equipped with a BL7 MAS probe and a high-power amplifier unit. Samples were placed in 7-mm ZrO_2 rotors. Sample spinning rates were 4.5 KHz for high-resolution spectra in the solid states, 1.7 KHz in the isotropic liquid state and in the slow spinning experiments for the spinning sideband study in the solid states. Typical decoupling power was ~50 KHz for the solid state and reduced to ~20 KHz for the liquid state; a duty cycle of ≤1% was used for all experiments. For crystalline samples, single-contact cross polarization from the H-1 reservoir to C-13 spins was employed to increase the C-13 sensitivity and shorten the effective C-13 relaxation time (Fyfe, 1983). The typical spin-lock field was ~50 KHz with the cross polarization transfer contact time of 1 ms and the pulse interval of 7 s. For the dephased CPMAS, a dephasing delay was inserted between the CP contact and the data acquisition to allow the C-13 signal decay through the C—H dipolar relaxation. The dephasing delays of 42, 50, and 150 μs were used to differentiate the molecular motions. For isotropic states, a standard single 90° (5 μs) pulse proton-decoupled C-13 MASNMR experiment was used, and the pulse interval was typically 7 s. The C-13 chemical shifts were all referred to the carbonyl carbon peak of glycine (176.06 ppm from $(CH_3)_4Si$) as an external reference. Spectra were typically obtained over 2K time domain points and were zero-filled to 8K, giving a spectral digital resolution of about 2.0 Hz. Sample temperatures were controlled to within ±1°C with the Bruker B-VT-1000 variable temperature unit. The probe temperature was calibrated as described before (Guo and Hamilton, 1993). Samples were allowed to equilibrate at desired temperature for 15–20 min before data acquisition.

X-ray powder diffraction patterns were recorded using nickel-filtered CuK-α radiation from an Elliot GX-6 rotating-mode generator (Elliot Automation, Borehamwood, UK) equipped with cameras using Franks double-mirror optics (Franks, 1958). The samples were packed into 1.0-mm diameter Lindeman capillaries (Charles Supper, Natick, MA), sealed, and examined in variable-temperature sample holders. The sample-film distance was calibrated by using the data of a standard material (crystalline cholesteryl myristate).

Differential scanning calorimetry experiments were carried out on a Perkin-Elmer DSC-7 (Norwalk, CT). Samples (1.5–5 mg) were sealed in a stainless-steel pan. An empty pan was used as a reference sample. Heating and cooling rates were 5°C/min. The machine was calibrated by using the data obtained for high-purity standard material (indium).

RESULTS

Identification of crystal forms of acylglycerols

Acylglycerols exhibit polymorphism because subtle differences in chain packing can be produced by varying the thermal history or the organic solvent for recrystallization. The phase transition temperatures for all the acylglycerols used in this work were measured by differential scanning calorimetry (Table 1). The melting temperatures for the corresponding acylglycerols available from the literature are listed for comparison. The α phase was readily identified because it formed from the isotropic (Iso) phase during cooling, and was characterized by lower melting temperatures compared with the solvent-recrystallized forms. It was difficult to identify β′ and β phases based on the melting behavior because they both recrystallize from organic solvents and the melting points are close to each other. Therefore, x-ray short-spacing data were measured for selected samples, MPG, DPG, and 1,3DMG, for identification of the phase (Lutton, 1950). The high-melting form of DPG was characterized by two strong diffraction lines at 4.21 and 3.80 Å, and high-melting forms of MPG and 1,3DMG were characterized by three strong diffraction lines at 4.27, 3.97, and 3.71 Å. These results satisfied the criteria for β′ phase (Larsson, 1966a). The low-melting form for all the acylglycerols has only one strong diffraction at 4.15 Å, corresponding to the α form (Larsson, 1966a). In addition, β, β′, and α phases are also characterized by triclinic, common orthorhombic, and hexagonal chain packing, respectively (Larsson, 1966a). Early MASNMR studies showed that triclinic chain packing was characterized by a C-13 chemical shift of 34.5 ppm for the interior methylenes of the acyl chains, substantially higher than any other chain-packing patterns (≤33.6 ppm, VanderHart, 1981). All the solvent-recrystallized crystalline forms used in this work gave a chemical shift in the region of 32.5–33.5 ppm (Table 2), for the interior methylenes, which clearly indicated that they were in β′ form instead of β phase.

General features of the C-13 spectra

1-monoacyl-sn-glycerol (MAG)

The C-13 MASNMR spectra of the Iso (liquid) and crystalline (α, sub-α, and β′) phases of MPG are shown in Fig. 1, *A–D*, respectively. The corresponding Iso, α, and β′ phases of MMG (not shown) gave the same spectral features as those in the MPG; there is no sub-α phase for MMG. In the Iso phase (Fig. 1 *A*), peak assignments for carbons in the acyl chain were based on the assignments of solution spectra of acylglycerols in the literature (Bociek et al., 1985). Carbons in the glycerol backbone (designated as G1, G2 and G3) were assigned by the following considerations. First, a DEPT

TABLE 1 The phase transition temperatures (°C) from DSC analyses

Compound	$T_{\beta'-l}$	$T_{l-\alpha}$	$T_{\alpha-\text{sub}-\alpha}$	$T_{\text{sub}\alpha-\alpha}$	$T_{\alpha-l}$
MMG	65.1, 67.5*, 70.5* (β)	49.5			52.8
MPG	77.46, 74.0*, 77.0* (β)	64.6	35.6	43.8	67.7
d-DMG	57.8, 59.0* (β)	34.9			38.1, 37.5*
r-DMG	55.6, 54*	34.2			37.9
DPG	70.2, 70.1‡	47.5			51.3
1,3DMG	67.6, 63.0*				

*Data from Small, 1986 ‡data from Kodali, 1990.

TABLE 2 Chemical shift values (ppm) of acyl glycerides in various phases

MMG				r-DMG			
Carbon	Liquid	α Phase	β′ Phase	Carbon	Liquid	α phase	β′ phase
G1	65.5	65.6	63.7(A), 63.0(B)	G1	62.8	63.5	62.6
G2	70.6	70.6	69.0, 67.9	G2	72.5	72.6	73.7
G3	63.8	63.9	61.4(B), 60.9(A)	G3	61.2	61.1	61.5
C=O	173.8	173.7	174.9(B), 172.9(A)	*sn*-1 (*sn*-3)-C=O	172.9	173.0*	175.5
C2	34.3	34.2	34.6	*sn*-2-C=O	172.8	173.0*	173.5
C3	25.2	26.1	26.6	C2	34.3, 34.1	34.2	35.5‡
C4–C10	30.1	32.9	33.5	C3	25.2, 25.1	26.4	27.8, 26.7
C11	29.7	32.6	33.5	C4–C10	30.1–29.7	32.8	32.6
C12	32.2	32.4	33.5	C11	29.5		
C13	22.9	23.9	25.1, 24.4	C12	32.2		
C14	14.1	14.3	15.0, 14.6	C13	22.9	24.2	24.6
				C14	14.1	14.2	14.9, 14.5

MPG					DPG			
Carbon	Liquid	α phase	sub-α phase	β′ phase	Carbon	Liquid	α phase	β′ phase
G1	65.5	65.6	64.0	63.7, 63.0	G1	62.8	63.5	62.6
G2	70.6	70.6	70.5	68.9, 67.8	G2	72.6	72.6	73.6
G3	63.8	63.9	64.3	61.3, 61.0	G3	61.3	61.2	61.4
C=O	173.8	173.6	173.6	174.9, 172.9	*sn*-1-C=O	172.9	173.0*	175.5
C2	34.3	34.2	34.2	34.6	*sn*-2-C=O	172.8	173.0*	173.3
C3	25.2	26.1	26.1	26.6	C2	34.4, 34.2	34.3	35.5‡
C4–C12	30.1	32.9	32.5	33.4	C3	25.2, 25.1	26.4	27.7, 26.7
C13	29.6	32.6	32.5	33.4	C4–C11	30.0–29.7	32.9	32.5
C14	32.2	32.6	32.5	33.4	C12	29.5		
C15	22.9	23.9	24.6	25.1, 24.0	C13	32.2		
C16	14.1	14.3	14.7	15.0, 14.6	C15	22.9	24.1	24.5
					C16	14.1	14.2	14.8, 14.4

d-DMG				1,3DMG		
Carbon	Liquid	α phase	β′ phase	Carbon	Liquid	β′ phase
G1	62.8	63.7	62.6	G1	65.3	66.7*
G2	72.5	72.5	73.6	G2	68.2	66.7*
G3	61.3	61.1	61.4	G3	65.3	66.7*
sn-1-C=O	172.9	172.8*	175.5	C=O	173.1	175.8 (1), 173.4 (3)
sn-2-C=O	172.8	172.8*	173.4	C2	34.2	
C2	34.3, 34.1	34.2	35.4‡	C3	25.2	27.3
C3	25.2, 25.1	26.3	27.8, 26.7	C4–C10	30.0–29.7	33.7
C4–C10	30.0–29.7	32.8	33.5	C11	29.5	
C11	29.5			C12	32.3	
C12	32.2			C13	22.9	25.7, 24.9§
C13	22.9	24.2	24.5	C14	14.1	15.1
C14	14.1	14.2	14.8, 14.4			

*Peaks superimposed on each other.
‡ There should be two C2 peaks belonging to *sn*-1 and *sn*-2 chains; it is likely that another one is buried under the broad signal of the main chain.
§ Tentative assignment.

(distortionless enhancement by polarization transfer) experiment (Harris, 1986) was used to detect the single-protonated carbon G2 (70.6 ppm) in the Iso phase (spectrum not shown). Of the two other glycerol carbon peaks, the peak at higher field (63.8 ppm) is tentatively assigned to be G3 assuming that the hydroxyl group provides stronger shielding than the ester group, and the peak at 65.5 ppm is thus assigned as G1. Assignments in the solid-state spectra were made by assuming that the chemical shifts of the solids correlate closely with those of the Iso state (Table 2). This assumption is usually true when the peaks in the solid state are well separated (Dalling et al., 1981), as in the current case.

Comparison of the spectra in Fig. 1 also shows the following important points. 1) In the Iso, α, and sub-α phases (Fig. 1, *A–C*), there is one peak corresponding to each carbon, whereas in the β′ phase there are two sets of peaks for several carbons, notably the C=O, G1, G2, G3, and ωCH_3 and $(\omega-1)CH_2$ carbons (Fig. 1 *D*); 2) the chemical shift of most carbons is dependent on the molecular arrangement, i.e., the shielding environment surrounding the individual carbon in each phase, and is thus characteristic of the phase; 3) the observed linewidths increase in the order of Iso < α < β′ ≪ sub-α phase; linewidth differences are greater for the protonated carbons (except for the CH_3) than for the nonprotonated carbons; 4) when the α or sub-α phase is converted into the β′ phase upon cooling, the new phase gives an identical spectrum as the β′ phase crystallized from organic solvent; 5) temperature changes did not affect the chemical shift or the linewidth

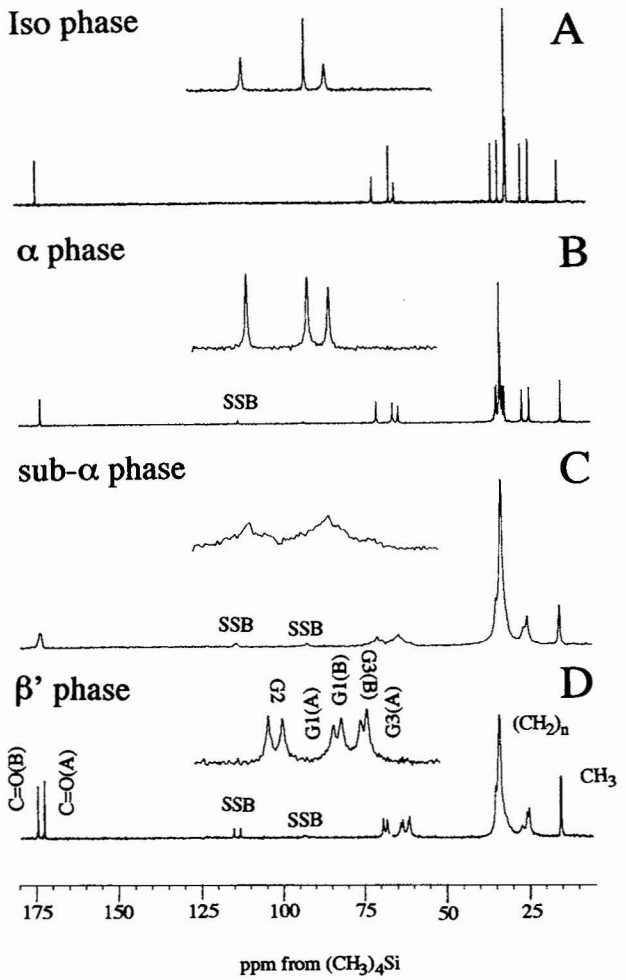

FIGURE 1 The C-13 MASNMR spectra of MPG in (*A*) Iso (80°C); (*B*) α crystalline (50°C); (*C*) sub-α, crystalline (25°C), and (*D*) β′ crystalline phases (25°C). Spectra of crystalline phases (β′, α, and sub-α) were obtained with a single-contact cross-polarization transfer experiment with the sample spinning 4.5 KHz at the magic angle. The spectrum for the Iso phase was obtained with a standard single-pulse proton-decoupled C-13 experiment with sample spinning 1.7 KHz at the magic angle. In all cases, a pulse interval of 7 s was used. All spectra were processed without line broadening (as in the following figures) after 400 scans. The same experimental conditions were maintained in Figs. 2 and 3.

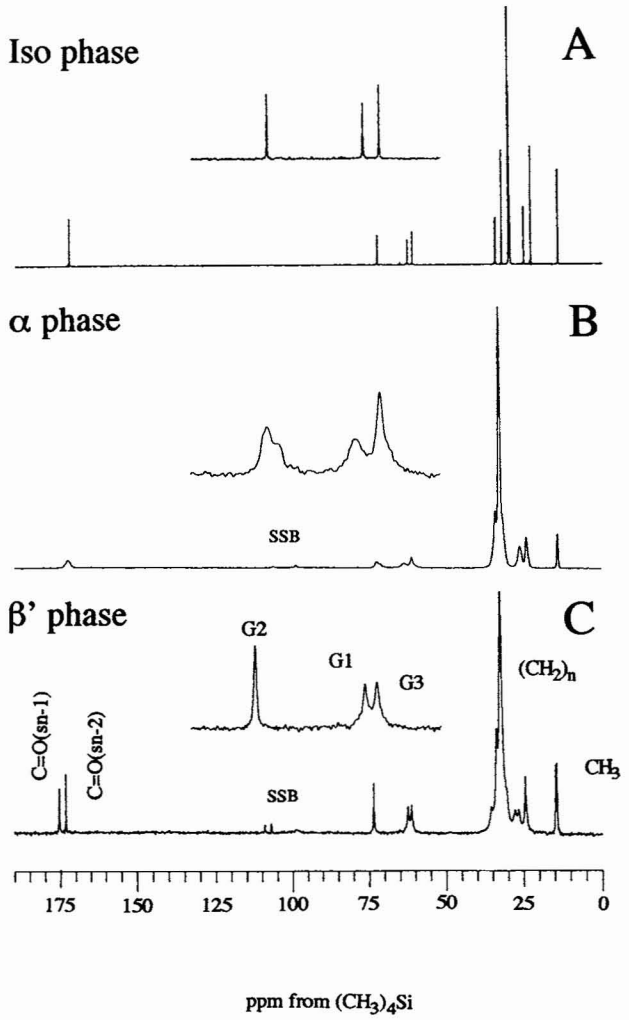

FIGURE 2 The C-13 MASNMR spectra d-DMG at (*A*) Iso phase (60°C), (*B*) α crystalline phase (30°C), and (*C*) β′ crystalline phase (25°C).

unless a phase transition occurred. These observations also apply to the diacylglycerols studied in this work.

1,2-diacylglycerol (1,2DAG)

Three different 1,2DAGs were studied in the present work: d-DMG, r-DMG, and DPG. The C-13 MASNMR spectra of the Iso, α, and β′ phases of d-DMG are shown in Fig. 2. Corresponding spectra of r-DMG and d-DPG were indistinguishable from those of d-DMG and are not shown. For r-DMG, the melting point of the hexane-recrystallized β′ form is about 2°C below that of the d-DMG (Table 1). The identical C-13 NMR spectra for that in the β′ phase of d-DMG and r-DMG suggest they have similar molecular packing patterns. Probably in the r-DMG, the d- and l-isomers are arranged in separated layers, and within each layer they are packed in the same pattern as that in d-DMG. The long spacing in β′ and α forms are 38.8 A and 44.4 A, respectively, for r-DMG (Howe and Malkin, 1951) and 39.1 ± 0.3 A and 43.4 ± 0.7 A for d-DMG (Kodali et al., 1990), also implying that r-DMG has the same crystalline structure as the individual isomers. For r-DMG, the α-Iso phase transition temperature is about that same as that in d-DMG, but as α phase melted, the recrystallization of β′ phase was not observed, probably because the nucleation and growth of the β′ structure within the α phase was hindered by the coexistence of d- and l-isomers.

The chemical shifts of these three 1,2DAGs are listed in Table 2. The peak assignments for carbons other than the C=O groups were made by the same strategy as for MAG and agreed with the reported assignments for DPG (Bruzik et al., 1990). From the Iso phase to α phase, every carbon peak broadened significantly (Fig. 2 *B*). Similar linebroadening in the α phase (compared with Iso or β′ phase) has also been shown in triacylglycerols (Bociek et al., 1985). In the β′ phase (Fig. 2 *C*), the corresponding peaks were narrower

than those in the α phase. For the d-isomers, the β' phase also formed when the α phase was melted (Albon and Craievich, 1990); the C-13 spectrum of the β' phase thus formed was the same as that recrystallized from hexane. The two methyl groups gave only one signal in the Iso and α phases, but in the β' phase they are observed as two individual peaks. The chemical shifts of the carbonyl resonances in the Iso phase agree with those reported previously (Hamilton et al., 1991a). The small separation between the *sn*-1 and *sn*-2 carbonyl carbons in the Iso phase (0.1 ppm) increased to ~2 ppm in the β' phase (Table 2); the two carbonyls were not resolved in the α phase.

The carbonyl carbons of d-DPG were assigned by adding DPG with C-13 enrichment of the *sn*-2 carbonyl to natural abundance d-DPG. The C=O peak at higher field in both Iso and β' phases was enhanced and thus assigned to the *sn*-2 C=O (Table 2). DPG at natural abundance gave a single broad C=O peak in the α phase, which was unaffected by addition of *sn*-2 C-13 enriched DPG. The assignment of *sn*-1 and *sn*-2 C=O peaks is assumed to be the same in other 1,2DAG.

1,3-diacyl glycerol (1,3DAG)

The C-13 MASNMR spectra of 1,3DMG in the Iso and β' phases are shown in Fig. 3, *A* and *B*, respectively. There is no α phase detected for this compound (Baur et al., 1949). The melting point of the β' phase formed from the melted Iso phase was 1–2°C lower than that of the β' phase crystallized from hexane because of subtle differences in the chain tilt angles (Kodali et al., 1990). However, the thickness of the glycerol region, obtained by extrapolating the long spacing versus the acyl chain length to the zero, is not significantly different in these two forms (Kodali et al., 1990). The C-13 resonances of these two β' forms were also identical.

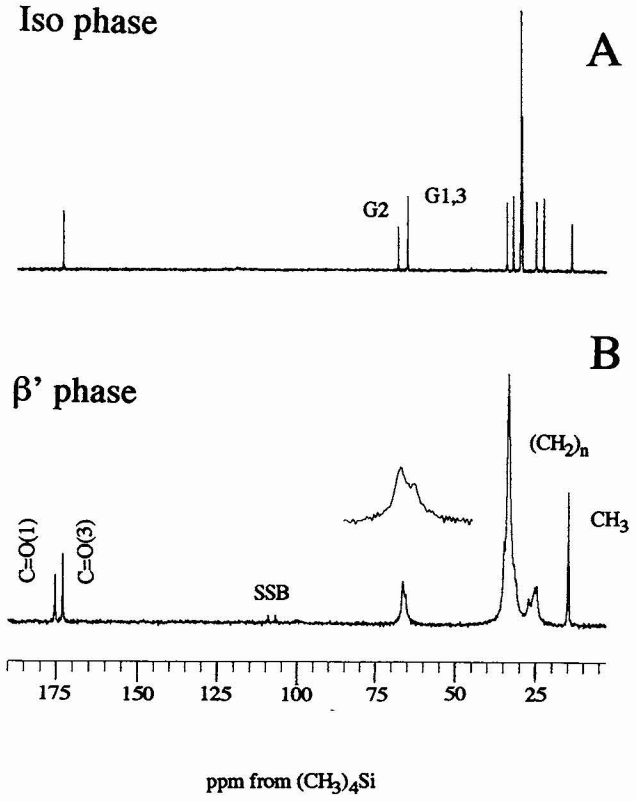

FIGURE 3 The C-13 MASNMR spectra 1,3-DMG in the (*A*) Iso phase (70°C) and (*B*) β' crystalline phase (25°C).

In the Iso phase, the chemically equivalent carbonyls and glycerol carbons gave single peaks (Fig. 3 *A*). In the β' phase, the two chains become structurally inequivalent, and separate peaks were observed for the two C=O groups (Fig. 3 *B*). The three glycerol backbone carbons all merged into one broad, asymmetrical peak. Peak assignments were made as described above; the chemical shifts and assignments are listed in Table 2.

Dephased CPMAS spectra

In a dephased CPMAS experiment, the decoupler is switched off for a short delay time between the end of the contact pulse and the start of the signal acquisition. During the delay, the C-13 magnetization decays most rapidly for carbons that are strongly dipolar-coupled to protons. Since the C—H dipolar interaction depends on r_{CH}^{-3}, the nonprotonated carbons (e.g., C=O) are less affected by the dephasing delay. Mobile carbons such as the ωCH_3 will also be less affected because the local dipolar field is significantly reduced by the rapid internal motions. Figs. 4 and 5 give the dephased CPMAS spectra of MPG, d-DMG and 1,3DMG in different phases. The spectra for MMG and MPG were the same. Spectra d-DPG and r-DMG were the same as that for d-DMG (not shown). In all cases, the C=O and ωCH_3 peaks were not significantly affected by the dephasing delay ($\leq$150 μs), whereas the other carbons were affected differentially, depending on their relative mobility.

For the β' phase, a dephasing delay of 42 μs completely suppressed peaks from the glycerol carbons in MPG (Fig. 4 *A*), d-DMG (Fig. 4 *B*) and 1,3DMG (Fig. 4 *C*), implying that the glycerol backbone is very rigid in all three cases. Silimar results were found for MMG, r-DMG, and DPG. A small residual signal from the acyl chains was observed for MPG (Fig. 4 *A*) and 1,3DMG (Fig. 4 *C*) but not for d-DMG. These residual acyl chain signals were completely suppressed when the dephasing period was 50 μs (Figs. 4, *D* and *E*). Therefore, the acyl chains are also very rigid, but the mobility increases slightly in the order of d-DMG < 1,3DMG < MPG.

Fig. 5 shows the dephased CPMAS spectra for MPG and d-DMG in the α phase, as well as MPG in sub-α phase. The same characteristics were observed for MMG, r-DMG and DPG, respectively. For MPG, all peaks are observed with a 42-μs delay period (Fig. 5 *A*). The peak intensities from the G1 carbon and the acyl chain are significantly reduced compared with those without a dephasing delay (Fig. 1 *B*), whereas G2 and G3 carbons are much less affected. With a 150-μs dephasing delay, all the protonated carbon peaks were further suppressed, but G1 and the acyl chain carbons were much more suppressed than G2 and G3 carbons (Fig.

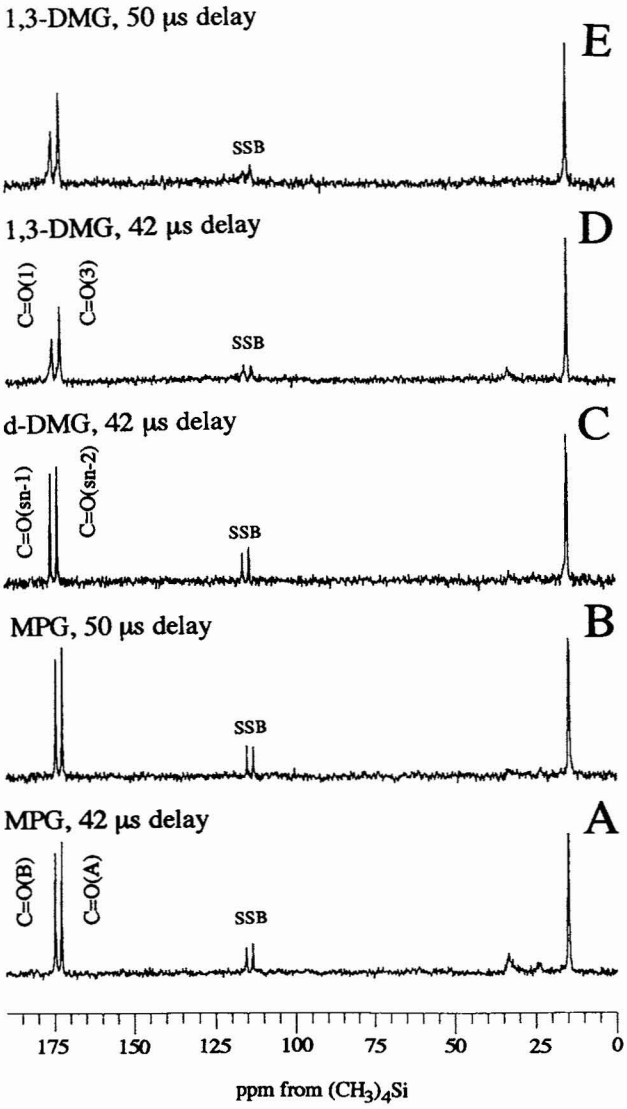

FIGURE 4 The dephased CPMAS spectra of acylglycerols in the β' phase (25°C): (*A*) MPG, with a 42-μs dephasing delay; (*B*) MPG, 50 μs; (*C*) d-DMG, 42 μs; (*D*) 1,3-DMG, 42 μs; (*E*) 1,3-DMG, 50 μs. The number of scans was 1K for each spectrum; other conditions are the same as shown in Fig. 1.

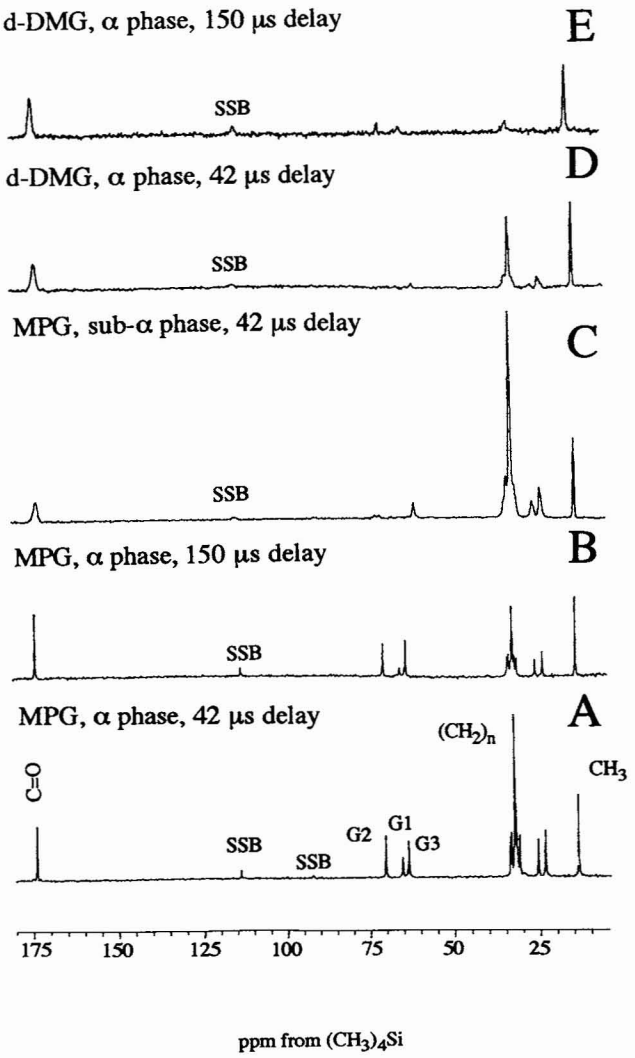

FIGURE 5 The dephased CPMAS spectra of acylglycerols in the α phase or sub-α phase: (*A*) MPG (α phase at 50°C) with a 42-μs dephasing delay; (*B*) MPG (α, at 50°C), 150 μs; (*C*) MPG (sub-α, at 25°C), 42 μs; (*D*) d-DMG (α, at 30°C), 42 μs; (*E*) d-DMG (α, at 30°C), 150 μs. The number of scans was 1K for each spectrum, other conditions are the same as in Fig. 1.

5 *B*). In the sub-α phase, except for the C=O and ωCH_3, all peaks were almost completely suppressed with a 42-μs delay period (Fig. 5 *C*), as for the β' phase.

In the α phase of d-DMG (and r-DMG, DPG; spectra not shown), a 42-μs delay completely suppressed peaks from G1 and G2 to an indetectable level, but not those from G3 and the acyl chains (Fig. 5 *D*), implying that G1 and G2 carbons are more rigid than G3 and the other acyl chain carbons. Increasing the delay time to 150 μs further suppressed these peaks; notably, peaks G3 and C3 almost completely disappeared (Fig. 5 *E*). Therefore, d-DMG molecules have an overall higher mobility in the α phase than in the β' phase, but a lower mobility than MPG in its α phase. The acyl chains of d-DMG are incorporated into the hexagonal sublattice; this appears to immobilize the G1 and G2 carbons and significantly reduce the mobility of G3 carbon (compared with the unesterified glycerol backbone carbons G2 and G3 in MPG). The characteristic features of these dephased CPMAS spectra in both β' and α phases are not significantly affected by increasing the temperature (spectra not shown).

Chemical shift anisotropies (CSA) of the carbonyl carbons in the acylglycerols

The carbonyl carbons of acylglycerols are located in key positions within the molecule, and knowledge of their chemical shift tensors can provide detailed information about molecular conformation. However, this information is removed by fast MAS as performed above. The nonspinning solid-state spectrum yields a powder pattern that carries the information of CSA, but such a spectrum usually exhibits a very low signal-to-noise ratio for carbon nuclei with large

CSA values. As an alternative method, with slow MAS spinning, high-resolution spectra can be obtained with the center peak flanked on both sides by sidebands spaced at the spinning frequency. The chemical shift tensors can be recovered from the intensity distribution of the spinning sidebands (Herzfeld and Berger, 1980).

Fig. 6 shows the slow-spinning MAS spectra of the carbonyl carbon of the acylglycerols. For MPG in the β' form, there are two center peaks for the carbonyl carbons representing the crystallographically nonequivalent molecules as described above, each flanked by its own spinning side band (SSB) pattern (Fig. 6 *A*). With nonspinning solid-state NMR, the two nonequivalent carbonyl carbons would not be resolved, and accurate CSA values could not be determined. In the α phase of MPG, only one center peak is observed for the carbonyl carbon, and with slow MAS, it is also flanked by its SSB (Fig. 6 *B*). For MMG, 1,2DAG and 1,3DMG in the β' phase, spectral features of the carbonyl peaks with slow MAS were similar to those of β' phase MPG (Fig. 6 *A*) and are thus not shown. For the α phase of d-DMG (as well as r-DMG, DPG), signals from the two chemically nonequivalent carbonyl carbons are observed as one broad peak, also flanked by its SSB (Fig. 6 *C*).

The three chemical shift tensors ($\sigma_{11} < \sigma_{22} < \sigma_{33}$), the chemical shift anisotropy ($\Delta\sigma = \sigma_{33} - \sigma_{11}$), and the ρ factor [$\rho = (\sigma_{11} + \sigma_{33} - 2\,\sigma_{22})/(\sigma_{33} - \sigma_{11})$] were calculated by fitting the individual intensities of the SSB to functions of chemical shift parameters (Herzfeld and Berger, 1980). The results are listed in Table 3 *A* (the β' phase at 25°C), Table 3 *B* (the α phase at 25°C), and Table 3 *C* (β' phase at different temperatures). Inspection of data in Table 3 shows 1) the absolute values of $\Delta\sigma$ values for all the crystalline acylglycerols are relatively large ($\geq$100 ppm); 2) for the β' phase of MAG, for which carbonyl signals are seen for the crystallographically inequivalent molecules, the $\Delta\sigma$ of the up-

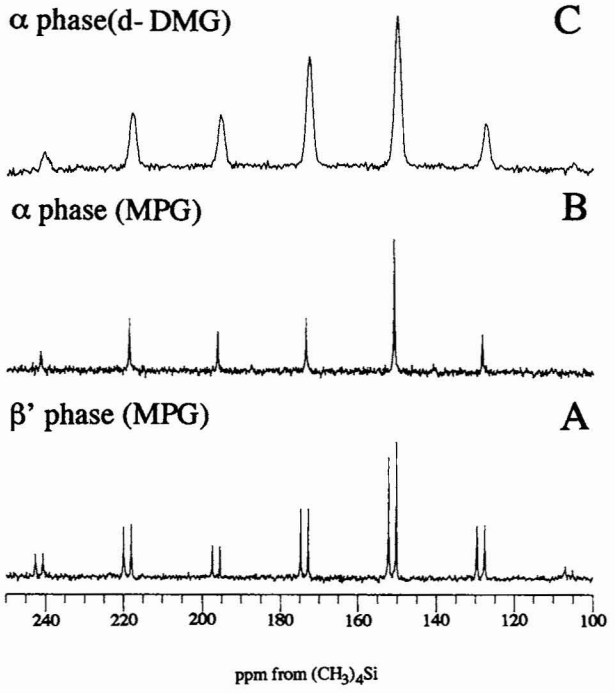

FIGURE 6 Carbonyl region of the slow spinning CPMAS spectra of (*A*) MPG, β' phase (25°C); (*B*) MPG, α phase (50°C); and (*C*) d-DMG, α phase (30°C). The spinning rate was 1.7 KHz and number of scans was 1K; other conditions are the same as shown in Fig. 1.

TABLE 3 The chemical shift tensors (ppm) of the carbonyl carbon in the acylglycerols (error ~ 10%)

(*A*) β' phase at 25°C

Compound	σ11	σ22	σ33	Δσ	ρ
MMG C=O(B)	130.7	140.0	254.0	122.9	0.85
C=O(A)	132.2	133.4	253.3	121.1	0.98
MPG C=O(B)	127.5	132.7	264.5	135.0	0.92
C=O(A)	129.0	129.2	260.4	131.4	1.00
d-DMG *sn*-1	114.2	159.3	253.0	138.7	0.35
sn-2	108.8	154.2	257.5	142.8	0.38
DPG *sn*-1	116.4	157.6	252.6	136.2	0.40
sn-2	115.2	157.4	247.7	132.4	0.36
r-DMG *sn*-1(*sn*-3)	113.8	157.9	254.8	141.0	0.37
sn-2	110.5	154.7	255.0	144.4	0.39
1,3DMG C=O(1)	124.2	144.3	258.0	133.8	0.70
C=O(3)	131.6	134.1	254.8	123.3	0.97

(*B*) α phase at 25°C

Compound	σ11	σ22	σ33	Δσ	ρ
MMG	127.9	129.9	263.2	135.5	0.97
MPG	134.9‡	134.9‡	251.0‡	116.2‡	0.99‡
	120.0*	141.2*	260.3*	140.3*	0.70*
d-DMG	126.9	147.5	244.0	117.1	0.65
DPG	132.1	150.6	253.8	103.7	0.65
r-DMG	128.4	147.1	243.0	114.6	0.67

(*C*) β' phase at different temperatures

	σ11	σ22	σ33	Δσ	ρ
MMG C=O(B)					
25°C	130.7	140.0	254.0	123.2	0.85
44°C	126.4	139.9	255.0	128.6	0.80
52°C	133.2	138.3	254.1	120.0	0.92
58°C	134.9	136.8	253.0	118.2	0.97
MMG C=O(A)					
25°C	132.2	133.4	253.3	121.1	0.98
44°C	131.5	131.6	255.5	124.0	0.99
52°C	133.1	134.8	250.8	117.6	0.97
58°C	133.4	135.0	250.4	117.0	0.99
d-DMG *sn*-1					
25°C	114.2	159.3	253.0	138.7	0.35
41°C	117.8	154.0	254.8	137.0	0.47
47°C	127.6	146.3	252.6	124.9	0.70
53°C	133.1	145.4	248.2	117.5	0.79
d-DMG *sn*-2					
25°C	108.8	154.2	257.5	142.8	0.39
41°C	112.1	154.0	254.0	141.9	0.41
47°C	113.2	148.9	258.0	144.8	0.51
53°C	114.1	149.4	256.7	142.6	0.51
1,3DMG C=O(1)					
25°C	124.2	144.3	258.0	133.8	0.70
45°C	122.2	147.6	256.8	134.6	0.62
56°C	122.6	146.2	257.7	135.1	0.65
1,3DMG C=O(3)					
25°C	131.6	134.1	254.8	123.2	0.97
45°C	131.5	133.8	255.1	123.6	0.96
56°C	131.6	132.3	256.9	125.5	0.99

*Data belong to the sub-α phase, 25°C

‡ Data acquired at 50°C.

field C=O peak is axially symmetrical, whereas the downfield peak is axially asymmetrical at 25°C, but approaches axial symmetry as the temperature is increased; 3) for the β' phase of 1,3DMG, for which two carbonyl signals are seen for the same molecule, the $\Delta\sigma$ of the upfield C=O peak is also axially symmetrical, but the downfield one is axially asymmetrical and does not change significantly as the temperature is increased; 4) for the α phase of MMG and MPG, only one C=O peak is observed, and the $\Delta\sigma$ is axially symmetrical; however, for MPG in sub-α phase, the C=O peak is broad, $\Delta\sigma$ is axially asymmetrical; and 5) for d-DMG, r-DMG, and DPG, $\Delta\sigma$ values are similar to each other, and are all axially asymmetrical in both β' and α phases.

DISCUSSION

1-monoacyl-*sn*-glycerol

The high-resolution MAS spectra of crystalline MMG and MPG provide information about both the crystal structural organization and molecular motions. In the β' phase, two sets of carbon signals in the glycerol moiety (G1, G2, G3, and C=O) and the terminal carbons ($(\omega-1)CH_2$ and ωCH_3) are seen (Fig. 1 *D*). The twin peaks represent the two crystallographically nonequivalent molecules, as previously observed for other lipids (Guo and Hamilton, 1993). Assuming that MAG has the same structure as the 1-mono-*sn*-glycerol of 11-bromoundecanoic acid in the β' phase (Larsson, 1966b), two symmetrically nonequivalent molecules (A and B) in the β' phase of MMG and MPG are expected. Such an assumption is generally acceptable, because compounds with the terminal methyl groups replaced by bromine atoms often crystallize isotypically with the corresponding unsubstituted compounds. A slightly greater chain tilt is sometimes required for the bromine-substituted glycerides in order to accommodate the bulky bromine atom (Kodali et al., 1990). Assignments of NMR signals to the nonequivalent molecules can be made by reference to the single-crystal x-ray diffraction data. The differences in orientation and chemical bond length between molecules A and B are slight but significant, as described in the literature (Larsson, 1966b). Since the carbons in the glycerol moiety are all directly bonded to oxygen atoms, which have the largest electronegativity in the molecule, in each twin set the more shielded (upfield) resonance is assigned to the carbons with shorter C—O bond length (Table 2). Such an assignment is straightforward for C=O and G1 because they are located inside the layered structure surrounded by hydrocarbons. Since G2 and G3 are located at the interlayer region and involved in the H-bonded network to maintain a head-to-head molecular arrangement (Fig. 7 *A*), their shielding is more susceptible to the through-space interactions by the surrounding nonbonded oxygens. The substantial chemical shift differences between the two signals for G2 indicates that the internuclei distances between G2 and its surrounding nonbonded oxygens must be significantly different in the A and B molecules. Rigorous assignments would require knowledge of the conformation of each OH group in the nearest neighbor of G2 and G3.

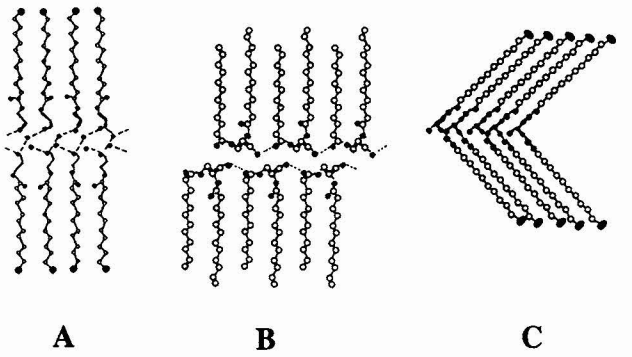

FIGURE 7 The crystalline structures of various acylglycerols or closely related derivatives in the β' phase obtained by single-crystal x-ray diffraction: (*A*) 1-*sn*-monoacylglycerol, (Larrson, 1966); (*B*) 1,2-dipalmitoyl-*sn*-glycerol, (Pascher et al., 1981); (*C*) 1,3–11-Br-diundecanoyl-glycerol (Hybl and Dorset, 1971). (○) Carbon atoms; (•) Oxygen atoms. Protons are not shown; the Br atoms in (*A*) and (*C*) are also shown (●).

The observation of two signals for the terminal carbons $(\omega-1)CH_2$ and ωCH_3 implies that one chain is extended farther outside the layer than its nearest neighboring chains. Because the terminal group in the model compound is modified by a bromine nucleus, a definitive single-crystal study of a long-chain MAG with an even number of carbons is needed to understand the precise molecular arrangement in the terminal region. The carbon signals from the interior methylenes of the acyl chain for both A and B molecules are superimposed and give a chemical shift value of 33.5 ppm, which agrees closely with the values observed for *n*-alkanes packed in the common orthorhombic sublattice (33.6 ppm, VanderHart, 1981).

A comparison of the chemical shift values of β' phase with those in the Iso liquid is also informative as to structural and dynamic features of crystalline MMG and MPG. On going from the β' to the Iso phase: 1) the inequivalence between molecules A and B of the crystal is lost and all the twin signals for the same carbon (e.g., C=O, G1, G2, G3, $(\omega-1)$-CH_2 and ωCH_3) merge into a single signal; 2) the intermolecular hydrogen bonding network, which results in the ordering and close packing of the glycerol moiety in the β' phase and causes a larger shielding on G1, G2, and G3 carbons, is disrupted, and the signals for the glycerol carbons move downfield by 1.6–3.0 ppm; 3) the all-*trans* conformation of the acyl chain in the β' form is replaced by random conformations undergoing fast *trans-gauche* exchange, and upfield shifts for the $(CH_2)_n$ as well as the $(\omega-1)CH_2$ and ωCH_3 resonances are seen; 4) the C=O peak in the Iso phase resonates between the twin peaks observed in the β' phase. According to Larsson (1966b), the planes through the C=O groups are twisted by 5° and 19° for molecules A and B in the β' crystal from the corresponding planes through the zigzag chains, so that the C=O bond in A is more compressed (1.19 A) than in B (1.25 A). Therefore, C=O (A) is more shielded. In the Iso phase, the intermediate bond length (1.23 A; Weast, 1972) might produce an intermediate chemical shift.

Single-crystal data for the α phase of monoacylglycerol were not available, but x-ray powder diffraction studies show hexagonal packing of the acyl chains with nonspecific chain-chain interactions. The thickness of the head groups, the projected length of the interior methylene groups, and the tilt angle appear to be very similar for the β' and the α phases (Kodali et al., 1985). However, the C-13 chemical shifts of the glycerol region (e.g., C=O, G1, G2, G3, C2) are almost identical in the Iso and the α phases and different from the β' phase (Table 2). In addition, corresponding peaks are only slightly broader in the α phase compared with the Iso phase (Fig. 1). These NMR results demonstrate that all molecules in the α phase are symmetrically equivalent, and that the glycerol region must be loosely packed, with considerably more disorder and mobility than in the β' phase (Small, 1986).

The Iso phase of MAG contains domains of bilayers of about 300 Å as revealed by x-ray scattering (Small, 1986). Such bilayers are more loosely arranged than the crystal and fast exchange of molecules occurs between domains; the acyl chains are completely disordered, but still maintain head-to-head aggregation, a remnant of the structural features of the α phase (Kodali et al., 1985). This explains the similarity of the chemical shifts of the glycerol region between the α and Iso phases. In the α phase, the chemical shift of the interior methylenes of the chain (C4–C12, 32.6 ± 0.3 ppm) is between that of the β' and the Iso phase. A similar chemical shift was observed in other lipids with hexagonally packed hydrocarbon chains (Meulendijks et al., 1989). Compared with the Iso phase, the downfield shift of the C3 and $(\omega-1)CH_2$ resonances in the α phase is likely to be caused by the chain-packing effect, and the terminal methyl was not affected due to its high mobility.

The mobility of monoacylglycerol molecules in crystalline phases can also be analyzed by comparison of the dephased CPMAS spectra with the normal CPMAS spectrum. Whereas linewidths may contain contributions from chemical shift inhomogeneity and other sources besides molecular motions, the dephased CPMAS experiment is directly related to the rotating frame relaxation time $T_{1\rho}$; a resonance with a short $T_{1\rho}$ is suppressed with a short dephasing delay. Although $T_{1\rho}$ contains contributions from both spin-spin and spin-lattice interactions, the former is the most important in the crystalline structures such as the β', sub-α, and α phases under current investigation (Fyfe, 1983). Spin-spin interactions between C-13 and H-1 are dominated by dipolar coupling that is dependent on the molecular motions. In the β' phase, the peaks for all the glycerol carbons are completely suppressed with a short dephasing delay (42 μs, Fig. 4 *A*). The peaks for the acyl chain (except ωCH_3), which are barely observable, are completely suppressed by extending the delay to 50 μs (Fig. 4 *B*). In the α phase, the signal decay rate (Fig. 5 *A*) is much less compared with that in the β' phase (Fig. 4 *A*), implying that the molecules in the α phase are more mobile that those in the β' phase. Similar observations that the glycerol backbone carbons are more rigid than the acyl chain carbons and that molecules in the β' phase are more rigid than in the α phase have been also reported for some triacylglycerols (Bociek et al., 1985). In addition, within the individual molecule in the α phase, signal suppression is in the order G1 > $(CH_2)_n$ (n = 2–13) > G2 ≈ G3. Such an observation shows that the G1 carbon and the acyl chain attached to it are less mobile than the G2 and G3 carbons, implying that the mobility of G1 is restricted by the ordered chain packing. Since G2 and G3 are quite mobile in the α phase (with slow dipolar relaxation; Fig. 5, *A* and *B*), it is unlikely that these carbons are involved in any stable intermolecular H bonding. The spectral features of the sub-α phase of MPG are very different from that of both α and β' phases. Although each carbon has a single signal, every peak is broad, especially the glycerol backbone signals (Fig. 1 *C*). Each molecular segment is rigid (except ωCH_3), as shown by the nearly total suppression of the signals with 42 μs in the dephased CPMAS spectrum (Fig. 5 *C*). The structure of this sub-α phase is unknown, but it is more ordered than the α phase, and its mobility is comparable to that in the β' phase.

1,2-diacyl glycerol

The molecular conformation of DPG in β' crystals determined by x-ray (Pascher et al., 1981) is shown in Fig. 7 *B*. There are two identical molecules per unit cell; therefore, only one C-13 signal is expected and observed (Fig. 2 *C*). The molecules are arranged in a bilayer structure, with the acyl chains aligned parallel and packed in the common orthorhombic sublattice; the acyl chain stacking is achieved by a bend in the initial part of the acyl chains. The chemical shift (32.5 ± 0.2 ppm) of the interior methylenes of the acyl chain (C4–C12) is about 1 ppm upfield from that observed in *n*-alkanes (VanderHart, 1981) or in MAG (Table 2) packed in the same type of sublattice. Such an upfield shift is due in part to stronger interchain dipolar interactions in 1,2-diacylglycerides (interchain distance of 4.88 A, Pascher et al., 1981) compared with MAG (interchain distance of 5.16 A, (Larsson, 1966b)). Additionally, acyl chains in 1,2DAG (Fig. 4 *C*) are more rigid than those in MAG (Fig. 4 *A*), which results in an increase in shielding and a lower chemical shift.

The glycerol moieties of 1,2DAG are laterally linked by intermolecular H bonding between the hydroxyl group on G3 carbon and the carbonyl oxygen on the *sn*-1 chain on an adjacent molecule. From the Iso to the β' phase, the chemical shifts of G1 and G3 are not changed, whereas the G2 peak moves downfield by about 1 ppm. This suggests that G1 and G3 experience no significant shielding change in the β' packing compared with the Iso phase. The lack of change in the shielding for G3 could be explained by a persistence of strong H bonding at the OH attached to G3 in the Iso phase. H bonding of liquid 1,2DAG was also suggested by analyses of the isotropic chemical shift in different solvent systems (Hamilton et al. 1991b). The downfield shift of G2 is likely due to the increase of C···O distances in the β' phase. Since the *sn*-2 ester group is buried inside the bilayer, and the distances between G2 and the surrounding oxygen atoms (the OH and the two carbonyl oxygens) are maximized, the

shielding from the oxygen dipoles is reduced, compared with that in the Iso phase. For similar reasons, the shielding on the two carbonyl carbons is also reduced in the β' phase compared with the Iso phase (Table 2). The chemical shift of the two carbonyl carbons in the β' phase can also be explained with reference to the crystal structure (Fig. 7 *B*). The *sn*-2 C=O is buried among the rigid *sn*-1 hydrocarbon chains, whereas the *sn*-1 C=O is located at the interface and involved as an electron donor in the H bonding. Therefore, *sn*-1 carbonyl carbon is less shielded and resonates downfield of the *sn*-2 carbonyl carbon (Table 2).

The C3 methylenes from the two chains also exhibit different chemical shifts in the β' phase (Table 2), reflecting a different environment, as expected from the crystal structure (Fig. 7 *B*). The *sn*-1 C3 is more shielded and assigned to the upfield signal. From Fig. 2 *C*, it is also apparent that all the methylene peaks (e.g., G1, G3, C3, etc.) are broader than those of the nonprotonated (C=O), single protonated (G2), and the terminal CH_3 groups. Similar differential linebroadening was evident in the CPMAS spectrum of DPG reported before, although not discussed (Bruzik et al., 1990). Such linebroadening is observed for other crystalline lipids (Guo and Hamilton, 1993), and is due to the less efficient decoupling for the methylene carbons caused by interference between the dipolar coupling and the decoupling field frequency.

There are no precise single-crystal data of 1,2DAG in the α phase. X-ray and electron diffraction patterns of DPG were more closely matched by several phospholipid structures (Fig. 8) than by the β' DPG structure (Dorset and Pangborn, 1988). Among these model phospholipids, the rotation about the G2—G3 bond is not restricted, but the inclination of the axis of the G2—G3 bond with respect to the layer normal is dependent on the phosphate headgroup size (Pascher et al. 1981). Such differences are induced by the size and orientation of the headgroup dipole; otherwise, the conformation of the diacylglycerol moiety is very similar in both DMPC molecules and is similar to that of 1,2-dilauroyl-*sn*-glycero-3-phosphatidylethanolamine (DLPE) (Shipley, 1986).

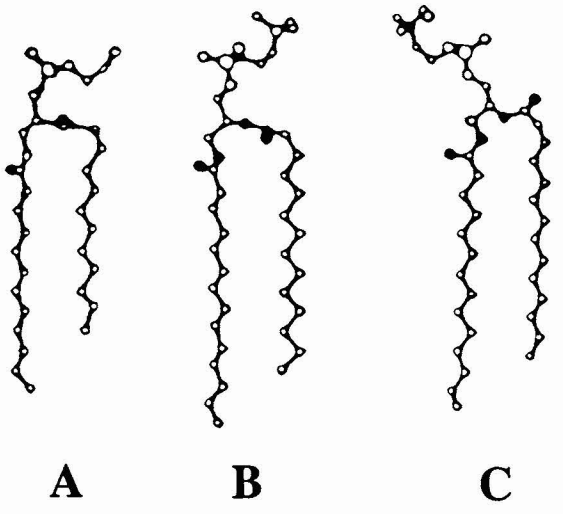

FIGURE 8 Model structures for 1,2-*sn*-diacylglycerol in the α phase: (*A*) DLPE (Shipley, 1966); (*B*). DMPC, conformation I, (Pearson and Pascher, 1979); and (*C*) DMPC conformation II, (Pearson and Pascher, 1979). Representations of atoms are the same as in Fig. 7.

The acyl chains of 1,2DAG in the α phase are packed in a hexagonal sublattice (Dorset and Pangborn, 1988), and the chemical shift of the interior methylene peak is the same as that of MAG in the α phase, which is similarly packed. However, the linewidth of this peak is much greater than that of MPG in the α phase. In addition, in the α phase of 1,2DAG, 1) G1 is shifted 1 ppm downfield, and G2, 1 ppm upfield (G3 does not change) relative to the β' phase, consistent with the hypothesis that the glycerol moiety adopts different conformations in these two crystalline phases (Dorset and Pangborn, 1988). In the β' phase the chemical shifts of G1 and G3 are about the same as those in the Iso phase, but G2 is about 1 ppm shifted downfield mostly because of the location of this carbon is inside the bilayer. In the α phase, G2 and G3 are located at the interface and give about the same chemical shifts as those in the Iso phase, whereas G1 is located inside the bilayer and is about 1 ppm downfield shifted because of the changes of the magnetic susceptibility in the local environment; 2) the two intrinsically inequivalent *sn*-1 and *sn*-2 C=O carbons are seen as one broad peak, probably because the difference in their chemical shifts is small compared with the linewidth in the α phase; 3) there is a shoulder on the right side of the G2 peak, implying that there is more than one signal for this carbon; 4) all carbons (especially those for C=O, G1, G2, C3 carbons) give broad linewidths compared with those in β' phase (Fig. 2). Although the linewidths of d-DMG (α phase) are close to those of MPG in its sub-α phase, the molecules are more mobile as indicated by the dephased CPMAS spectra, implying different linebroadening mechanisms; 5) the linewidth of the carbons in the glycerol backbone follows the order G2 $\approx$ G1 > G3.

Compared with the β' phase, molecules in the α phase are packed more loosely with no stable intermolecular H bonding (Dorset and Pangborn, 1988). The differential linebroadening observed for G1, G2, and G3 peaks is less likely to be related to the mobility than a distribution of chemical shifts (Adebodun, et al., 1992); i.e, the observed peaks (G1 and G2) represent the average signal of several different conformations in intermediate exchange (10^{-5}-10^{-3} s^{-1}), whereas the free rotation about the G2—G3 bond allows the shielding on G3 to be highly averaged to give a narrow peak. These results suggest that the glycerol backbone may actually undergo constant reorientations among a few different but closely related conformations, of which those shown in Fig. 8, A-C have larger probabilities. The shoulder on the upfield side of the G2 peak might correspond to conformation(s) other than those represented by the mean peak.

The dephased CPMAS spectra of 1,2DAG in the β' phase show that all carbons except the terminal CH_3 are rather rigid. By comparison, in the α phase all carbons (except G1 and G2) are quite mobile, consistent with the above interpretation of linewidth data. This observation agrees with the assumption that the linebroadening in the α phase is a result of several coexisting conformations.

1,3-diacyl glycerol

In the β' crystalline structure, the molecules are packed in a triclinic lattice with T parallel subcells and the acyl chains extended on both sides of the glycerol moiety (Fig. 7 *C*, Hybl and Dorset, 1971). The two carbonyl groups are inequivalent and give different C-13 resonances, and the G1 and G3 also become inequivalent (Fig. 3 *B*). The inequivalence of the peak heights originates from the large difference in the corresponding CSA values (Table 3). Since the O—C=O (1) is H bonded with the OH on G2 of its nearest lateral neighbor, (Fig. 7 *C*), the redistribution of electron density through the H bonds results in a downfield shift of the corresponding O—C=O (1) (175.8 ppm) and an upfield shift of the G2 carbon (see below). The O—C=O (3) is not involved in the H bonding, and its resonance shifted only slightly downfield compared with that in the Iso phase. Other changes that occur during crystallization, such as changes in conformation, mobility, and interchain distance, might also affect the shielding, although to a much lower and less straightforward extent. In the glycerol backbone, G1 and G2, but not G3, are affected by the intermolecular H bonding. The formation of H bonds increases the shielding on G2 but has less effect on G1 and G3 (Table 2). Because the resonances of G1, G2, and G3 are close to each other in the β' phase, they appear to be a broad and asymmetrical signal centered at 66.7 ppm. Another factor that might contribute to the linebroadening is the disordering of the glycerol moiety (Hybel and Dorset, 1971). However, this effect is small and contributes to only a small distribution of chemical shifts and hence, an apparent linebroadening. In the Iso phase, fast molecular motions narrows the resonance and the nonequivalence of the two acyl chains is lost. Only one C-13 signal was observed for each carbon as expected (Fig. 3 *A*).

For the interior methylenes of the acyl chains, the chemical shift is usually dependent on the chain-packing symmetry. In the current case, the C-13 chemical shift of the interior methylenes (33.7 ppm, Table 2) is lower than that for *n*-alkane in triclinic lattice (34.9 ppm, VanderHart, 1981), but the same as for (1,2-*sn*-dihexadecylglyceryl)silatrane, whose acyl chains also exist in a triclinic lattice (33.67 ppm, Meulendijks et al., 1989). Strong intermolecular interactions through the dipole-dipole interaction of the bulky polar head groups [1,2-*sn*-dihexadecylglyceryl)silatrane] or through H bonds (1,3-diacylglycerol) should make the acyl chains less mobile in these lipid crystals than those in the *n*-alkane crystals, leading to a greater shielding and lower chemical shift.

CSA

Because the carbonyls of acylglycerols are located in a key region of the molecule and their interactions help determine molecular conformations, we studied the carbonyl region in greater detail by CSA measurements. The breadth of the anisotropy signal ($\Delta\sigma$) is related to the sizes and orientations of the three principle tensors, which is in turn related to the motional modes. As shown in Table 3, $\Delta\sigma$ values for the C=O carbon in all the acylglycerols studied are ~100 ppm, which implies that the molecules in their crystalline states are undergoing some type of anisotropic motion that is fast compared with $\gamma H_o \Delta\sigma \approx 10^4\ s^{-1}$ (Wittebort et al., 1981). However, since the $\Delta\sigma$ values for the acylglycerols are all of the same order of magnitude, the parameter of $\Delta\sigma$ itself is not sufficient to differentiate the mobilities of the acyl chains in different acylglycerols in different phases of the same molecule or in the same phase at different temperatures.

When analyzed in terms of the axial asymmetrical factor $[\rho = (\sigma_{11} + \sigma_{33} - 2\,\sigma_{22})/(\sigma_{33} - \sigma_{11})]$, the CSA data yield information about the differential mobility provided that the conformation is known. By definition, when $\rho = 1$, the shift tensor is axially symmetrical ($\sigma_{11} = \sigma_{22} \neq \sigma_{33}$). Since two of the components are identical but different from the third, a "unique axis" is implied; i.e., σ_{33} (also called $\sigma_\parallel$); correspondingly, $\sigma_{11} = \sigma_{22}$ axes are called $\sigma_\perp$ (Griffin, 1981). A full breadth of the carbonyl CSA is 148 ppm (Wittebort et al., 1981; Smith et al., 1992). For an axially symmetrical tensor, the residual CSA ($\Delta\sigma_R$) is related to the static anisotropy ($\Delta\sigma_s$) by

$$\Delta\sigma_R = \Delta\sigma_S\,(3\cos^2\theta - 1)/2 \qquad (1)$$

where θ is the angle between the unique shielding tensor axis and the axis of motion (Wittebort et al., 1981; Griffin, 1981). When $\rho \neq 1$, $\sigma_{11} \neq \sigma_{22} \neq \sigma_{33}$, Eq. 1 is no longer applicable, and there is no simple correlation between the observed CSA and the molecular motional effect on the conformation of unique axis.

In the β' phase, MAG shows two C=O peaks reflecting the two crystallographically nonequivalent molecules. The upfield C=O peak (A molecule) gives $\rho(A) \approx 1$, but the downfield peak (B molecule) gives $\rho(B) \neq 1$. As the temperature is increased in the β' phase, $\rho(A)$ does not change, whereas $\rho(B)$ increases to approach to the value of $\rho(B) \approx 1$. This change of $\rho(B)$ from axial asymmetry to axial symmetry probably reflects a change in the conformation of the ester group. Because the ester groups are not involved in the H bonding, a limited change in the conformation might take place, causing ρ to approach the axial symmetrical value. As mentioned above, in the β' phase at 25°C the planes through the carboxyl group in molecule B are twisted by 19° from the corresponding plane through the zigzag chains. As the temperature approaches the β'-isotropic phase transition temperature, it is possible that the crystalline structure expands and the carboxyl group in molecule B is gradually untwisted. The conformation of A may also change, but not as significantly as that in B. From Eq. 1, the calculated angle between the unique shielding tensor axis ($\sigma_\parallel$) and the axis of motion in molecule A is about 21 ± 2°, and increases only very slightly as the temperature increases. The angle for molecule B at high temperature also falls into this range.

In the α phase of MAG, all molecules are equivalent, and the $\Delta\sigma$ of the C=O peak at 25°C is slightly larger than those in the β' phase. Because acyl chains pack differently in the

α and β' phases, resulting in a difference in the conformations of the ester groups, the CSA data for these two different phases cannot be compared in a quantitative manner. By using Eq. 1, the angle between the unique shielding tensor axis ($\sigma_{\parallel}$) and the axis of motion in the α phase is calculated to be about 14°.

For the three 1,2-diacylglycerols studied in this work, the breadths of the CSA for C=O carbons in the β' phase were significantly larger than those for MAG, and close to the value of the full breadth (148 ppm). Since the CSA for both *sn*-1 and *sn*-2 C=O carbons are axially asymmetrical ($\rho \ll 1$), Eq. 1 is not applicable, and additional theoretical and experimental work would be required to determine the conformation. In the α phase, the observed breadth of CSA is smaller, but still with $\rho \ll 1$. However, the observed broad signal might be the result of chemical exchange, and it is not presently possible to interpret the observed CSA unambiguously.

For 1,3DMG in the β' phase, the upfield peak (representing the C=O that is not H bonded) gives $\rho \approx 1$, but the downfield peak (C=O that is H bonded) gives $\rho \neq 1$; the CSA values of both C=O groups are not significantly affected by temperature. The conformation of the H-bonded C=O is strongly restricted, and that of the other C=O is not as strongly restricted. In both cases, the increase in temperature did not cause detectable conformation effects on the carbonyl carbons.

SUMMARY

Various polymorphic phases of three types of acylglycerols, MAG, 1,2DAG, and 1,3DAG, have been studied by MAS-NMR. All phases show a single peak for each carbon except the β' phase of MAGs, which show two peaks for each carbon, corresponding to the two crystallographically nonequivalent molecules. The chemical shifts are dependent on the specific polymorphic phase, and the chemical shift differences between different phases were interpreted in terms of changes in the intramolecular bond distance, intermolecular interactions (such as H bonding), and molecular motions. For MAG, linewidths of corresponding resonances follow the order of isotropic phase < α < β < sub-α; for 1,2 DAG linewidths were narrower in the β than in the α phase. The linewidths of MAG reflect relative mobility in the different phases, whereas the greater linewidth of the α phase of 1,2 DAG is probably caused by the coexistence of several slightly different conformations. Dephased CPMAS spectra in the β' phase show that the glycerol backbones of MAG, 1,2DAG and 1,3DAG are quite rigid; acyl chains are also rigid, but the mobility differences were detected: 1,2DAG < 1,2DAG < MAG. Dephased CPMAS spectra in the α phase show a greater mobility of MAG than 1,2DAG and significant motions in parts of each molecule, in contrast to the β' phase.

The chemical shift anisotropy of the carbonyl signals in each acylglycerol was measured by slow spinning MAS-NMR. It was found that for MAG in the β' phase, one molecule undergoes a conformational change as the sample temperature approaches the melting point, while the other molecule remains fixed in conformation. The carbonyl CSA in the α phase is axially symmetrical, with a similar quantity as that in the β' phase. For the 1,2DAG, the C=O is axially asymmetrical in both β' and α or sub-α phases. For the 1,3DAG, the two acyl chains are nonequivalent in the β' phase: the H-bonded carbonyl gives an axially asymmetrical CSA, and the non-H bonded, an axially symmetrical CSA.

The authors thank Dr. S. P. Bhamidipati for the *sn*-2 C-13 enriched 1,2-dipalmitoyl-*sn*-glycerol provided. We also thank Dr. S. O. Smith for the critical reading of the manuscript and helpful discussions.
Supported by RO1 HL41904 from the National Institutes of Health.

REFERENCES

Adebodun, F., J. Chung, B. Montez, E. Oldfield, and X. Shan. 1992. Spectroscopic studies of lipids and biological membranes: carbon-13 and proton magic-angle sample-spinning nuclear magnetic resonance study of glycolipid-water systems. *Biochemistry.* 31:4502–4509.

Albon, N., and A. Craievich. 1986. Thermal study of phase transitions of dipalmitoyl 1,2-glyceride. *J. Phys. Chem.* 90:3434–3436.

Baur, F. J., F. L. Jackson, D. G. Kolp, and E. S. Lutton. 1949. The polymorphism of saturated 1,3-diglycerides. *J. Am. Oil Chem. Soc.* 71:3363–3366.

Bociek, S. M., S. Ablett, and I. T. Norton. 1985. A ^{13}C-NMR study of the crystal polymorphism and internal mobilities of the triglycerides, tripalmitin and tristearin. *J. Am. Oil Chem. Soc.* 62:1261–1266.

Bruzik, K. S., G. M. Salamonczyk, and B. Sobon. 1990. ^{13}C CP-MAS study of the gel phases of 1,2-dipalmitoylphosphatidylcholine. *Biochim. Biophys. Acta.* 1023:143–146.

Chapman, D. 1962. The polymorphism of glycerides. *Chem. Rev.* 62: 433–456.

Dalling, D. K., K. W. Zilm, D. M. Grant, W. A. Heeschen, W. J. Horton, and R. J. Pugmire. 1981. A solution and solid carbon-13 magnetic resonance study of the conformation of 9,10-dihydroanthracene and its 9,10-methylated derivatives. *J. Am. Chem. Soc.* 103:4817–4824.

De Boeck, H., and R. Zidovetzki. 1992. Interactions of saturated diacylglycerols with phosphatidylcholine bilayers: a ^{2}H NMR study. *Biochemistry.* 31:623–630.

Di, L., and D. M. Small. 1993. Physical behavior of the mixed chain diacylglycerol, 1-stearoyl-2-oleoyl-*sn*-glycerol: difficulties in chain packing produce marked polymorphism. *J. Lipid Res.* 34: 1611–1623.

Dorset, D. L., and W. A. Pangborn. 1988. Polymorphic forms of 1,2-dipalmitoyl-*sn*-glycerol: a combined x-ray and electron diffraction study. *Chem. Phys. Lipids.* 48:19–28.

Epand, R. M., R. F. Epand, and C. R. D. Lancaster. 1988. Modulation of the bilayer to hexagonal phase transition of phosphatidylethanolamines by acylglycerols. *Biochim. Biophys. Acta.* 945:161–166.

Franks, A. 1958. Some developments and application of microfocus x-ray diffraction techniques. *Br. J. Appl. Physics.* 9:349–352.

Fyfe, C. A. 1983. Solid State NMR for Chemists. C.F.C. Press, Ontario.

Ganong, B. R., C. R. Loomis, Y. A. Hannun, and R. M. Bell. 1986. Specificity and mechanism of protein kinase C activation by *sn*-1,2-diacylglycerols. *Proc. Natl. Acad. Sci. USA.* 83:1184–1188.

Griffin, R. G. 1981. Solid state nuclear magnetic resonance of lipid bilayers. *Methods Enzymol.* 72:108–174.

Guo, W., and J. A. Hamilton. 1993. Molecular organization and motions of cholesteryl esters in crystalline and liquid crystalline phases: a ^{13}C and ^{1}H magic angle spinning NMR study. *Biochemistry.* 32: 9038–9052.

Hamilton, J. A., S. P. Bhamidipati, D. R. Kodali, and D. M. Small. 1991a. The interfacial conformation and transbilayer movement of diacylglycerols in phospholipid bilayers. *J. Biol. Chem.* 266: 1177–1186.

Hamilton, J. A., D. T. Fujito, and C. F. Hammer. 1991b. Solubilization and localization of weakly polar lipids in unsonicated egg phosphatidylcholine: a ^{13}C MAS NMR study. *Biochemistry.* 30:2894–2902.

Harris, R. K. 1986. Nuclear Magnetic Resonance Spectroscopy: A Physicochemical View. Longman Scientific and Technical, Essex, U.K.

Herzfeld, J., and A. E. Berger. 1980. Sideband intensities in NMR spectra of samples spinning at the magic angle. *J. Chem. Phys.* 73: 6021–6030.

Howe, R. J., and T. Malkin. 1951. An x-ray and thermal examination of the glycosides. Part XI. The 1:2-diglycerides, and further observations on 1:3-diglycerides *J. Chem. Soc.* 2663–2667.

Hybl, A., and D. Dorset. 1971. The crystal structure of the 1,3-diglyceride of 11-bromoundecanoic acid. *Acta Cryst.* B27:977–986.

Kodali, D. R., D. A. Fahey, and D. M. Small. 1990. Structure and polymorphism of saturated monoacid 1,2-diacyl-*sn*-glycerols. *Biochemistry.* 29:10771–10779.

Kodali, D. R., T. G. Redgrave, D. M. Small, and D. Atkinson. 1985. Synthesis and polymorphism of 3-acyl-*sn*-glycerols. *Biochemistry.* 24:519–525.

Larsson, K. 1966a. Classification of glyceride crystal forms. *Acta Chem. Scand.* 20:2255–2260.

Larsson, K. 1966b. The crystal structure of the L-1-monoglyceride of 11-bromoundecanoic acid. *Acta Cryst.* 21:267–272.

Lutton, E. S. 1950. Review of the polymorphism of saturated even glycerides *J. Am. Oil Chem. Soc.* 27:276–281.

Meulendijks, R. H. W. M., J. W. De Haan, M. H. Van Genderen, and H. M. Buck. 1989. Conformational transmission in condensed lipid model compounds. *Eur. J. Biochem.* 182:531–538.

Norton, I. T., C. D. Lee-Tuffnell, S. Ablett, and S. M. Bociek. 1985. Calorimetric, NMR and x-ray diffraction study of the melting behavior of tripalmitin and tristearin and their mixing behavior with triolein. *J. Am. Oil Chem. Soc.* 62:1237–1244.

Pascher, I., S. Sundell, and H. Hauser. 1981. Glycerol conformation and molecular packing of membrane lipids. *J. Mol. Biol.* 153:791–806.

Pearson, R. H., and I. Pascher. 1979. The molecular structure of lecithin dihydrate. *Nature.* 281:499–501.

Shipley, G. G. 1986. X-ray crystallographic studies of aliphatic lipids. *In* Handbook of Lipid Research. The Physical Chemistry of Lipids: From Alkanes to Phospholipids. Plenum Press, New York. 97–147.

Siegel, D. P., J. Banschbach, and P. L. Yeagle. 1989. Stabilization of H_{II} phases by low levels of diglycerides and alkanes: an NMR, calorimetric, and x-ray diffraction study. *Biochemistry.* 28:5010–5019.

Small, D. M. 1986. Handbook of Lipid Research: The Physical Chemistry of Lipids: From Alkanes to Phospholipids. Plenum Press, New York. 672 pp.

Smith, S. O., I. Kustanovich, S. Bhamidipati, A. Salmon, and J. A. Hamilton. 1992. Interfacial conformation of dipalmitoylglycerol and dipalmitoylphosphatidylcholine in phospholipid bilayers. *Biochemistry.* 31:11660–11664.

Soulages, J. L., M. Rivera, F. A. Walker, and M. A. Wells. 1994. Hydration and localization of diacylglycerol in the insect lipoprotein lipophorin. A ^{13}C-NMR study. *Biochemistry.* 33:3245–3251.

VanderHart, D. L. 1981. Influence of molecular packing on solid-state ^{13}C chemical shifts: the *n*-alkanes. *J. Magn. Res.* 44:117–125.

Weast, R. C. 1972. CRC Handbook of Chemistry and Physics, 52nd ed. CRC Press, Boca Raton, FL. F173.

Wittebort, R. J., C. F. Schmidt, and R. G. Griffin. 1981. Solid-state carbon-13 nuclear magnetic resonance of the lecithin gel to liquid-crystalline phase transition. *Biochemistry.* 20:4223–4228.